Accepted Manuscript

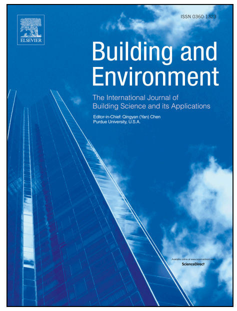

Stone weathering under Mediterranean semiarid climate in the fortress of Nueva Tabarca island (Spain)

J. Martínez-Martínez, D. Benavente, S. Jiménez Gutiérrez, M.A. García-del-Cura, S. Ordóñez

PII: S0360-1323(17)30220-2

DOI: 10.1016/j.buildenv.2017.05.034

Reference: BAE 4924

To appear in: *Building and Environment*

Received Date: 27 March 2017

Revised Date: 12 May 2017

Accepted Date: 24 May 2017

Please cite this article as: Martínez-Martínez J, Benavente D, Jiménez Gutiérrez S, García-del-Cura MA, Ordóñez S, Stone weathering under Mediterranean semiarid climate in the fortress of Nueva Tabarca island (Spain), *Building and Environment* (2017), doi: 10.1016/j.buildenv.2017.05.034.

Stone weathering under Mediterranean semiarid climate in the fortress of Nueva Tabarca island (Spain)

Martínez-Martínez, J.[1,2,*], Benavente, D.[1], Jiménez Gutiérrez, S.[3], García-del-Cura, M.A.[4], Ordóñez, S.[1]

[1] Departamento de Ciencias de la Tierra y del Medio Ambiente. Universidad de Alicante. Campus San Vicente del Raspeig. 03690 San Vicente del Raspeig (Alicante, Spain).

[2] Instituto Geológico y Minero de España (IGME). Calle Ríos Rosas, 23. 28003 Madrid (Spain)

[3] Instituto de Ecología Litoral. C Santa Teresa, 50. 03560 El Campello (Alicante, Spain).

[4] Instituto de Geociencias (IGEO) (CSIC-UCM). C José Antonio Novais, 12. Ciudad Universitaria 28040 Madrid (Spain)

* Javier.martinez@igme.es

Abstract

The Nueva Tabarca fortress constitutes an exceptional example of baroque architectural heritage. However, the aggressiveness of the local environment and the low suitability of the used building stone cause their fast deterioration. The hydro-mechanical properties of the building stones, the characteristics of their porous system (open porosity and pore size distribution), the global climate of the island and the particular microenvironmental conditions of each studied monument explain the weathering process acting on the porous limestone of Nueva Tabarca.

Results reveal that Halite crystallization and wind erosion are the main weathering agents. On the one hand, wind plays a critical weathering action because it controls the salt crystallization process, the abrasion by wind-blown particles, as well as the wind-driven rain impact. Different weathering forms are related to each erosion mechanism. On the other hand, the relative humidity in the island determines the agressiveness of the halite crystallization process. Salt damage activity was calculated quantifying not only the number of halite crystallization-dissolution transitions, but also the duration of the driest periods.

Finally, a novel parameter (Equivalent Years, Y_{eq}) is defined in order to quantify the representativeness of standarized artificial ageing tests. Y_{eq} expresses the number of years of natural ageing required for achieving the same weathered state of rocks after laboratory procedures. A wide range of Y_{eq} values are obtained for the studied rocks (from 8 to 165 years), showing a strong dependency with both the exposure time as well as the agressiveness of the environment.

Key words: porous limestone, calcarenite, halite, aeolian erosion, salt crystallization,

1. Introduction

Porous limestones probably constitute the most important stone resource as building material in the architectural heritage of the coastal cities of the southwestern Mediterranean region. Tens of historic sites were built using this type of rock due to their workability, aesthetic appeal and availability. Some representative examples are: the use of Sabucina stone in Sicily

(Italy) [1]; Apulia calcarenite in SE Italy [2]; Ksour Essaf limestone in Tunisia [3]; Globigerina limestone in Malta [4]; Marés stone and Santanyí stone in Mallorca (Spain) [5-6]; and San Julián stone and Bateig stone in Alicante (Spain) [7]. In this framework, the unfinished baroque fortress of Nueva Tabarca island (SE of Spain), and the local calcarenite used for its construction, constitutes an exemplary study case.

The dry mediterranean climate prevails in the coastal zones of this region and it is characterized by hot and dry summers and mild and wet winters. In marine semiarid conditions, it is thoroughly accepted that the main deterioration process is related to salt crystallization [8-10]. However, different mechanisms for marine salt supply are proposed including capillar uptake, saline rainwater incursion, condensation and evaporation of atmospheric humidity, or dry deposition of marine aerosol [8, 10-12].

Stone weathering in natural environments is complex and it is correlated with many different physicochemical processes operating both sequentially and synergistically [13]. Swelling during wetting-drying cycles, mineral chemical dissolution and deterioration by thermal expansion are considered as active decay processes that can act simultaneously to salt weathering [10, 12, 14]. However, wind contribution to the stone decay is scarcely treated in bibliography, although it is an important environmental factor controlling the salt crystallization process [9, 15-16], erosion by wind-blown solid grains [17], and wind-driven rain impact [18].

The type and rate of weathering of stones depend somewhat on the geographical building location and on the stone location within the architectural structure [10]. However, stone decay resistance is mainly due to their hydro-mechanic properties in terms of water absorption, capillarity or mechanical strength [2], which are dependent, in turn, on the porous system of the rock.

The objective of this study is to understand the weathering process under marine semi-arid climatic conditions of the porous building rocks used in the architectural heritage of Nueva Tabarca Island. For this purpose, the different lithofacies were identified, their conservation state was quantified in situ and finally, they were sampled from the historic quarry for subsequent laboratory characterization. The influence of the local climate on the conservation state of each kind of rock is analysed tacking into account: i) the location of the monument inside the island; ii) the position of the stone block within the building; iii) the orientation with respect to wind; iv) the exposure period of the rock to the environment, and finally, v) the hydro-mechanical properties of the building stones and the characteristics of their porous systems. Results from laboratory tests have been compared with the in-situ conservation state of building materials focusing the analysis on the significance of the accelerated ageing tests with respect the observed natural rock decay.

Taking into account the cultural, artistic and touristic importance of the Nueva Tabarca village, its preservation and conservation are a major issue, both from cultural and economic points of view. This importance emphasizes the need to understand the environmental induced deterioration processes and the deterioration susceptibility of building stones in order to define future preservation and/or conservation strategies.

2. Materials and methods

2.1 Study site

Nueva Tabarca island (Alicante province, SE of Spain) is located at 22 km from Alicante city and 8 km from Santa Pola city (figure 1). The island has elongated shape (1800 m in length and 450 m in width) with a remarkable East-West orientation. A fortified settlement was founded in its western part in the 18th century.

The fortified village constitutes an exceptional example of homogeneous baroque architectural heritage [19]. The singularity of the monuments was recognized by means several local and national protective figures. The initial plans for this fortified city were focused in the building of a strong wall around the west part of the island and the construction of several buildings with military, religious and civil functions. The reason for this important intervention was to offer a stronger resistance against the Barbary pirates. The construction works began in the middles of 18th century, and in 1770 the works were stopped due to economical, political and logistic problems. The result was the construction of the most part of the wall, the church, the governor's house and a complex hydraulic system in order to supply the population with fresh water. Due to the insularity conditions, the building materials supply was restricted to the local resources. In this context, the rock with the best characteristics for ashlars carving and sculptural elements was a yellowish calcarenite which outcrops in one of the rocky islets surrounding the main island (*La Cantera* islet). However, despite of the fact that the whole rock blocks were extracted from the same local quarry, several lithofacies can be recognised and each one presents a different response against the weathering agents.

The aggressiveness of the local environment and the low suitability of the used building stone cause the fast deterioration of monuments. Several restorations on the walls and the church were carried out during 20th and 21st centuries. Two of the most important interventions were executed during the decade of 1970 and during the first decade of the present century. The first one was focused on the rebuilding of lost parts of the city-walls, including the reconstruction of the vaults of the city-wall entrances. Local and foreign building stones were used as reintegration materials. The later was focused mainly on the church, although some punctual repairs were also carried out on parts of the wall. Foreign building stones were exclusively used in this intervention despite of their significative aesthetic and textural differences with the local and original material.

The most emblematic elements of the local defense structure are the three main city-wall entrances. They are named *San Rafael*, *San Miguel* and *San Gabriel*, and they constitute the East, North and West entrance to the city, respectively (figure 1). The current work is focused on the study of these monumental city-wall doors. They were selected due to: i) the presence of different lithofacies as building stones with different weathering degrees; ii) the existence of both original and rebuilt parts in each monument, offering rock blocks with different exposure periods to the same evironmental conditions; iii) the different orientation of each city-wall door, which is related to different exposures to the main wind directions and to the amount of solar insolation; iv) the presence of historic graphic documents of these monuments which allow to distinguish both the original and the rebuilt areas.

2.2 Material characterizaton and alteration products

Six different lithofacies were recognised as building materials in the city-wall doors (AA1, AA2, AB1, AB3, C1 and C2) (figure 2). Differences between them were established according to: a) the content of lithoclasts; b) the type of bioclasts (mainly focused on the predominance of red algae or briozoans grains); c) the average size of components, and d) the presence/absence of sedimentary structures (lamination). Hand sample description was completed with microscope observations of thin sections under petrographic optical microscope (Assioscop Zeiss transmitted light microscope).

Studied rocks, as well as samples of salt efflorescences, subefflorescences and crusts were analysed by powder X-ray diffraction in a Philips PW-1710/00 diffractometer (Cu Kα radiation with a Ni filter and a setting of 40 kV and 40 mA). Data were collected and interpreted using the XPowder software package.

AA1 and AA2 correspond to well sorted lithoarenites (grain size between 150 and 400 µm) with abundant foraminifera. Lithoclast composition is quartz and rock fragments of both volcanic rocks and limestones. Main mineralogy corresponds to calcite and dolomite (contents of 60.59% and 25.02%, respectively). Quartz (5.88%), plagioclase (3.44%) and clays (5.06) are also present. AA2 shows preferred orientation of petrographic components at microscale and lamination is visible at hand sample observation.

AB1 is a very well sorted lithoarenite (mean grain size of 300 µm). Bioclast content is very low in this rock and they are restricted to small briozoa fragments and some foraminifera. Lithoclast composition is mainly limestone fragments. Carbonates constitutes the main mineralogy (85.92% of calcite and 8.30% of dolomite). Quartz grains can be also present (5.78%).

AB3 is fine-grained sandy calcarenite (grain size lower than 100 µm with some isolated big component ranging between 150 and 400 µm). Bioclast are mainly foraminifera and, subordinaterly, fragments of briozoa, red algae and echinoderms. Lithoclasts are mainly composed by rock fragments of both volcanic rocks and limestones, but some quartz grain can be also observed. Mineralogical content corresponds to calcite (71.69%), dolomite (15.18%), quartz (9.64%) and plagioclase (3.49%).

C1 and C2 correspond to calcirrudite with a high content of algal rhodolith (several centimetres in size), and, subordinately, briozoans and foraminifera. Differences between C1 and C2 are related to lithoclast content: high in C1 (mainly carbonate rock fragments) and very low in C2 (mainly quartz). C1 also shows a fibrous calcite crust cement rounding the grains. In both cases, the main minerals detected in global analysis are calcite (around 65.41%), dolomite (16.63%), quartz (7.75%) and plagioclase (3.16%).

All these varieties were identified and sampled in the local quarry for laboratory analysis.

2.3 In situ analysis of rock weathering

Conservation state analysis of studied city-wall doors was carried out at the mesoscale by visual inspection and monument mapping. Different deterioration patterns observed in rock ashlars were classified according to the criteria established by ICOMOS ICS glossary [20]. Two thematic maps were elaborated on these elements: lithology and erosion maps. The first one shows the rock varieties employed in each monumental door and their distribution. The erosion map represents the lost volume of rock ashlar. The lost volume was calculated measuring the distance between both the original and the current surface of each rock ashlar. The original surface was defined by means a steel bar supported on non-eroded areas close to eroded stones. Measurements were taken to the mean depth of the recessed surface. This parameter measures the depth to which weathering penetration has caused sufficient loss of integrity of the rock to permit disintegration or detachment of rock material. Similar methodology was applied in [21] and [22].

2.4. Climatic characterization

Nueva Tabarca island climate was measured by means of a weather station (Davis-Wireless Vantage PRO2) which included a tipping-bucket rain gauge (Davis 7852) for rainfall measurements, and a 12-bit smart Sensor (Davis 7315) to measure the relative humidity and air temperature with an accuracy of ± 0.5ºC above -7ºC, and ±2% from 10% to 100% RH. These parameters were recorded every 30 minutes from April 2009 to February 2011. The Data Acquisition System consisted of a WeatherLink (#6510) data logger. Unfortunatly, due to the corrosive environment of the island, lacks in the data register occur due to several electronic problems during the measurement period.

In addition, a manual termometer and hygrometer (Vaisala HMP75) was used in order to both calibrate the continuous recording and measure specific climatic conditions around the three studied monuments. Discrete measurements were carried out in autumn (18^{th} December), winter (15^{th}, 23^{rd} and 24^{th} January), spring (2^{nd} April) and summer (28^{th} July and 4^{th} August).

2.5. Rock properties characterization

A detailed study of the pore structure was carried out in terms of porosity and pore-size distribution. The open porosity (ϕ_O) was calculated using the vacuum water saturation test (after [23]). Pore size distribution was quantified by means of mercury porosimetry (MIP). The connected porosity (ϕ_{Hg}), the mean pore size (r_M), median pore size (r_{MD}) and bulk density (ρ_{bulk}) were obtained by Autopore IV 9500 Micromeritics mercury porosimetry. The pore size interval ranges from 0.002 to 200 μm.

Hydric properties of rocks were defined by means of capillar porosity (ϕ_{cap}) and both capillary and evaporation coefficients (C and E, respectively). The capillary coefficient is the sorptivity expressed in $kg/m^2h^{0.5}$ (according to [24]). The evaporation coefficient is also expressed in $kg/m^2h^{0.5}$ and corresponds to the slope of the curve representing the weight loss as a function of the square root of time. Rock strength was determined by means of the Point Load Test after the methodology proposed in [25].

Rock durability was estimated via a salt crystallization test. Five samples of each kind of lithofacies were tested and a 14 % w/w Na_2SO_4 solution was used, in accordance with the EN-12370 recommendations [26]. The dry weight loss (DWL) at the end of the 50 cycles of salt crystallization test was used to evaluate the resistance to salt weathering.

2.5.1 Modified Böhme abrasion test

In order to quantify the superficial resistance of rocks to the erosion by wind-blown particles, a modification of the standardized Böhme abrasion test is carried out [23]. The aim of the current modification is focused on the inability to obtain big samples from protected sites as it is required for the standardized methodology (samples of 71x71x71 mm).

The modified test employs small prismatic samples of 20x30x30 mm in size. The abrasion process is carried out in a plate grinding machine rotating at a speed of 30 cycles per minute with a solid steel counterweight applying a load of 0.02 N/mm^2. The load was applied to the sample and the disk was twirled for 15 minutes. Two perpendicular surfaces of the same sample were tested. The mBAL parameter (modified Böhme Abrasion Loss) is obtained from the volume loss calculated as (eq. 1):

$$mBAL = \Delta V = \frac{\Delta m}{\rho_b} \qquad \text{Eq. 1}$$

Where ΔV is the volume loss at the end of the test (in mm^3); Δm is the mass difference (in g); and ρ_b is the bulk density of the rock.

In order to check the validity of the modified Böhme test, nine ornamental stones were tested after both the new proposed test (four measurements per variety) and the standardized wide wheel abrasion test [23]. Selected rocks include porous and massive limestones, marbles, travertines and quarzites. Equation 2 expresses the relationship found between the values obtained by means of each procedure. A very good correlation exists between them (R^2=0.87).

$$mBAL = 8.9 \cdot T_{ww} - 86.5 \qquad \text{Eq. 2}$$

where *mBAL* is the value obtained by means of the modified Böhme Abrasion test, and T_{ww} is the trace measured in the rock after the Wide Wheel Abrasion test.

3. Results and discussions

3.1. Porous system and rock properties

Table 1 displays the results obtained for the pore structure and whole properties characterization of the rocks from monuments of Nueva Tabarca island. Figure 3 shows the pore size distribution of the studied rocks using the MIP method. All the studied varieties have a complex porous media characterized by high porosity (16.15-24.13%), although two groups can be recognised according to their pore-size distribution. On the one hand, the varieties AA1, AB1 and C1 have a polymodal distribution composed of several (two or three) pore families with radius defined in the whole detectable range of the MIP technique. On the other hand, AA2, AB3 and C2 present a main pore population centered in a narrow pore size range (1-5 µm for AA2, 0.2-1 µm for AB3 and 0.08-1 µm for C2).

Figure 4 shows the decay forms developed in the studied samples during the salt crystallization tests. Table 1 includes the mean dry weight loss at the end of the test, the kind of decay form observed and the cycle at it was first observed. Rock susceptibility to decay by salt crystallization is directly related to its pore size distribution. AA2 (DWL~23.43%), AB3 (DWL~78.59%) and C2 (DWL~20.53%) are revealed as very sensitives to salt crystallization. The rest of varieties remain almost unweathered at the end of the test (DWL<1%). The weakest rocks do not have the highest porosity value. For example, AB3 samples have the lowest porosity value and however, they are almost completely destroyed after the salt crystallization test. AB3 shows a significant weight loss although its porous system and the hydric properties are not different to the rest of rock varieties. As we mentioned above, the durability of a rock is controlled by its both pore size distribution and mechanical properties of the rock. AB3 is the softest variety (rock strength around 24.34 Mpa after the PLT), and consequently, the material's resistance to the mechanical action of salt crystallization is very low.

Water is one of the main factors involved in most of the weathering processes. Both the amount of water absorbed and the ability of the water transport are controlled by the pore space of the rock. Three regions can be distinguished depending on the transfer mechanism involved. Firstly, for pores ranging between 0.001 and 0.1 µm water will condense at relative humidity values below 99%. Further variations in the thermo-hygrometric conditions between stone surface and the air determine the amount of water within stone. Secondly, capillary suction is significantly relevant to materials for pore radius between 1 µm and 100 µm, constituting the so-called capillary pores [12,27-28]. Finally, gravitational flow occurs for pores with a diameter greater than 1 mm. The first two types are the main moisture transport mechanisms involved in rock deterioration, and the pore fractions associated to them has been marked in the MIP curves of figure 3. According to these limits, three pore subgroups are established: microporosity (including pores with radius lower than 1 µm), mesoporosity (radius between 1 and 100 µm) and macroporosity (pores with radius higher than 100 µm). More than the 50% of the pores contanied in the porous system of AA1, AA2, AB1 and C1 range between 1 and 100 µm (mesopores) and it is directly correlated to their high both capillar and evaporation coefficient. All these varieties are classified as highly absorbing rocks according to their C value (C>3.0 $kg/m^2h^{0.5}$) [29]. This absorbing behaviour is firstly unfavorable for rock durability due to the ease with which salty water can access to the inner part of rocks.

AB3, however, is on the opposite behaviour. Its content in mesopores is very low (9.75%) and consequently presents the lowest values of both capillarity and evaporation coefficients. On the contrary, the 90% of pores have radius lower than 1 µm, and around the 35% of them are included in the smallest ranges (r<0.1 µm). This pore causes moisture adsorption and condensation processes inside the stone. Therefore AB3 is prone to be intensely decayed, not only by salt crystallization as was discused above, but also by other weathering mechanisms related to high water retention such as: i) the development of microorganisms on the stone surface, ii) clay swelling; or iii) reduction in mechanical strength due to stone softening [12].

C2 shows an intermediate behavior between the two above discussed situations. The main pore population presents a moderate content of mesopores (radius between 1 and 100 µm) (20.98%) and a high content of pores with radius between 0.1 and 1 µm (65.82%). As a consequence, the hydric behavior of this rock variety varies between AB3 and the rest of rocks, showing values of C and E intermediate between them.

3.2. In-situ rock weathering

All the rock varieties were indiscriminately used in the construction of the city-walls. However, the presence of each one in the doors varies significately (figure 5). The original contruction of the eastern entrance shows a preferred used of AB3 (around 27% of the total stone volume used in the monument) and AB1 (19%). The northern entrance was originatelly built with similar quantities of AA2, AB1 and C1 (24%, 21% and 18%, respectively). AA2 was, however, the preferential rock variety used in the western entrance (43%), followed by C1 (17%). A randomly used of the rock varieties is also observed in the reconstruction works of the upper parts of the monuments. However, a preferential use of AA1 and AB1 is observed in the eastern entrance, AB3 and AA1 in the northern entrance and AB3 in the western one.

Despite of the fact that there are not an univocal relationship between the observed decay forms and the lithology where they are developed, some general correlations can be carried out. The deterioration of AA2, C2 and AB3 is by differential erosion. This decay pattern is developed eroding preferentially soft layers included in laminated structures (AA2, figure 6a), removing the soft matrix surrounding the hard filling of burrows (AB3), or eliminating the matrix surrounding hard fossil components (rhodoliths in C1, and especially in C2) (figure 6d and 6e). Furthermore, AB3 can show other decay patterns such as alveolization, especially in the upper parts of the monuments (figure 6b). Some examples of scaling can be found in AB1 (figure 6f). Finally, well-developed rounding forms take place preferentially in AB1 (figure 6c). All these weathering forms observed in monuments coincide with the results obtained in laboratory during the salt crystallization test (table 1 and figure 4), verifying the relevance of this mechanism in the Nueva Tabarca's monuments decay.

Figure 5 displays the conservation state of the rocks in the three studied monumental city-wall doors. The vertical erosion profile has been added to the erosion map of each door in order to show the maximum, medium and minimum measured recession depth at different heights.

Two different patterns results in each door. On the one hand, the eastern entrance (San Rafael Entrance) is the most weathered (maximum measured recession = 27.5 cm), showing an intensity decrease from lower to upper parts. On the other hand, northern entrance and western entrance (San Miguel and San Gabriel entrances, respectively) are much better preserved (maximum measured recession = 16.1 cm and 6.6 cm, respectively) and the highest recession depths are found in the upper parts. It is important to highlight that most of these upper areas correspond to the rebuilt volume of the monuments during the restoration works of 1975 (figure 1). These “inverse profiles” are explained by means of lithological and environmental factors. On the one hand, the rebuilt part of the eastern door took place with durable varieties preferentially (AA1 and AB1) whilst the weakest stones were used in the original ashalrs (AB3 and AA2). However, one of the most frequent replacement stone used in the northern and western doors was the softest variety (AB3). On the other hand, environmental factors control the different erosion intensity observed in each monument: i) the relative humidity and temperature of the island over the year; ii) the particular microclimate in each city-wall doors according to both their orientation and distance to the sea; and iii) the exposure of each façade to the wind. Moreover, the erosion agents act heterogeneously on the doors (especially in the case of the wind), contributing to the unlike erosion of the walls. All these aspects will be treated in depth in the next sections.

Table 2 shows the mean recession depth reached by each variety. Table 2 distinguishes the mean recession depths values of the original ashlars and the blocks added during restoration works (in 1975). In general, the most weathered variety is AB3, followed by AA2. It agrees with the durability registered by these rocks during the salt crystallization test. On the other hand, a high durability was assessed in laboratory for AA1 and C1 and it agrees with the current conservation state observed in the northern and western entrances. However, values obtained in AB1 and C2 do not show a homogeneous trend in the studied monuments. AB1 is the less eroded rock variety in the original stones of the eastern entrance (as it is expected according to the laboratory results), but shows a medium MRD value in the other two entrances. On the contrary, C2 (potential weak variety) presents a medium erosion degree in the original blocks of the eastern entrance and low MRD values in the northern city-wall door. These discrepancies can be explained attending, on the one hand, to the low use of C2 in the studied monuments; and on the other hand, to the different rock exposition to weathering agents which depends on its location inside the own monument.

3.3. Climatic control on salt crystallization

The local climate of the Nueva Tabarca island during the period April 2009 to February 2011, expressed as monthly averages, are shown in Table 3. A Mediterranean semiarid climate (“Csa” according to Köppen-Geiger climate classification) dominates the geographic area of the island, with an annual average temperature of 19.3ºC and a strong seasonality, with monthly temperature variations ranging between 12.3ºC (December) and 26.8ºC (August). The maximum temperature values were recorded during summer (from June to August) and range from 29.8 to 32.9ºC. The minimum temperature was recorded from December to February, reaching minimum values of 3.6ºC. The relative humidity was high due to the proximity of the sea, with an average annual value of 74.3%. The seasonal fluctuation was low, ranging the minimum relative humidity registered during the driest months (autumn-winter) between 30.2 and 32.5% and the minimum value during the wettest period (summer) of 50.3%. Maximum values close to 90% are always found in each month. Daily fluctuations, however, can be significative, moving from 80% to 40% during a 12 hours period.

The region is characterized by relatively low annual rainfall (251 mm during the registered period), in accordance with the prevailing semiarid climate. During summer, there are long periods of drought, with only short and punctual rainfalls. The maximum rainfall is in autumn and winter. Torrential rains are characteristic in this period. For instance some extreme 24 h rainfalls were recorded on 2 March 2010 (66.6 mm) and 27 January 2011 (44.3 mm).

Halite in different proportions was always found in the weathered rocks sampled from Tabarca's buildings and presents a powdery or fine-grained texture. Rock weathering by salt crystallization is considered one of the most important processes acting on the building stones in monuments under marine environments [9-10]. Salt crystallization occurs through different mechanisms closely related to changes in environmental conditions [30]. Salts with different hydrated phases (such as thenardite-mirabilite phases for sodium sulphate) are sensitive to both relative humidity and temperature. Non-hydrated salts, such as sodium chloride, crystallise at a fixed humidity virtually independent of temperature [31]. Halite can crystallise only when the ambient relative humidity is lower than its critical deliquescence point (75.3%). According to this assertion, several authors define the NaCl transitions as the number of times the average daily relative humidity crossed the critical deliquescence point of 75.3% on consecutive days [9, 31-32]. The number of transitions is virtually the number of crystallisation-dissolution cycles. However, [30] considered that only when the relative humidity is lower than 65.3%, evaporation in rock pores is important enough to cause high supersaturation and high crystallisation pressures. Thus, these authors suggest quantifying the transitions for NaCl by considering the number of times the relative humidity crossed the critical relative humidity of 65.3% on two consecutive days. Transition for NaCl in the Tabarca environment is calculated according to both criteria, and the number of times that the relative humidity is lower than each critical value has been expressed as ^{75}T and ^{63}T (table 3). Criteria proposed by previous authors are based on daily climatic records. We propose two different parameters that consider the high sampling frequency of the temperature and relative humidty of timeseries (every 30 minutes). On the one hand, $T_{0.5}$ counts the total number of times the relative humidity decreases below a threshold value (75.3% and 63.5% for $^{75}T_{0.5}$ and $^{63}T_{0.5}$, respectively) in the record. On the other hand, T_5 specifies how many cases of the previously quantified $T_{0.5}$, the relative humidity remains below the critical value during at least the sequent 5 hours. Moreover, the total number of hours per month in which the relative humidity is lower than the critical value is also quantified (table 3). All these calculated parameters can be classified in two groups: the transitions countings (T and $T_{0.5}$) and the duration estimators (T_5 and the number of hours). In the first ones, the length of the dry period is not relevant, whilst it is in the second group.

Figure 7 plots the climatic values recorded during the monitoring period. Two lines mark the critical values for halite crystallization (RH=75.3% and RH=63.5%). Figure 7 and Table 3 highlight the significant increase in the frequency of halite transitions at the end of autumn (November-December) and during winter (January-February). This increase is not only registered in the number of phase transitions but also in the duration of the periods in which the relative humidity is continuously under the critical values. This last aspect of the salt transition is crucial because it reflects the effectiveness of the water evaporation at the stone surface. Long dry periods remove a higher amount of moisture from the rock surface. Colston et al. [8] observe that the rate of stone decay achieved in extended periods where the ambient relative humidity is less than 75%, is higher than it is in areas where the cycling is relatively frequent. At the beginning of the evaporation process, liquid water is moved by capillary forces from the inside of the rock towards the surface. After that, when the water content in the rock is low, the capillary transport is completely replaced and controlled by water vapor conductivity processes [28]. When a partially satured rock is exposed to an evaporation period longer than 5 hours, the replacement of the moisture transport mechanism (from capillar to vapor transfer) can happen. As a consequence, salt crystallization will take place at or just below the stone surface, being possible the disintegration of superficial grains or the development of scales [9]. This process is more effective in areas moderately wet (instead of completely saturated), such as rocks located on the median-high parts of monuments where the supply of ground water to stone is limited, and it can explain, in part, the “inverse erosion profiles” observed in the northen and western city-wall doors (figure 5) where the upper part of the monument is more intensely decayed than the lower areas.

Therefore halite crystallization is the main responsible of stone weathering of the city-wall doors of Nueva Tabarca island, and it is more harmful at the end of autumn and during the winter. However, measurements of the microclimatic conditions at the specific environment surrounding the three studied city-wall doors showed that slight differences exist between them. Table 4 shows the temperature and relative humidity measured at different times and days along the studied period. Northern and western entrances resulted the wetest ones, registering the highest relative humidities. Eastern city-wall door, instead, is the dryest, and the relative humidity measured in this point is between 5 and 23% lower than it is in the other two entrances. This difference is due to the fact that northern and western entrances are the closest to the coastline (less than 10 m). As a consequence, especific salt transitions in the eastern entrance microclimate are expected to be more frequents and more prolonged than they are in the northern and western entrances. Environment surrounding the eastern city-wall door is therefore more aggressive from a salt crystallization point of view, and it agrees the higher erosion intensity measured in this façade.

According with climate projections for the Mediterranean area, a change in patterns of salt damage is expected due to the future intensification of dry conditions [33-34]. The warmer and drier trends in the Nueva Tabarca area involve a lesser frequency of salt transitions, but longer periods with RH values lower than critical values. Consequently, more effective conditions for salt crystallization are expected due to the major evaporation during the driest periods.

3.4. Aeolian erosion with and without wind-blown particles

Wind in coastal regions is an important weathering agent, especially due to both the ability for driving salty water deep into the fabric of building and the abrasive sand action that can saltate and erode materials [17,35]. However, this weathering agent is commonly unconsidered in heritage deterioration studies and even some authors consider wind erosion as an infrequent decay agent [36].

Table 5 summarizes the monthly averages of wind speed and wind direction in Nueva Tabarca Island during the studied period (April 2009 – February 2011), as well as the mean directions and number of hours of high-energy winds. Two preferential directions occur when all the data are considered (low, medium and high-energy winds) (Figure 8). On the one hand, eastern winds prevail during summer (from May to September), with directions ranging between N50E to N150E. On the other hand, W and WNW directions were preferentially registered from the end of autumn (November) to February. These preferential directions vary slightly when only the most energy winds were considered. In this case, the summer winds (from July to September) trended to blow with NE directions (between N40E and N65E), whilst the autumnal winds (from September to November) had SWS directions (ranging from N195E to N220E).

Two different kinds of pavements exist in front of the studied city-wall doors. The northern and western entrance have a small rocky terrace, whilst in the case of the eastern entrance, a large sandy area connect the village with the rest of the island. This fact determines two different situations of the city-wall doors in the face of wind-blown particle erosion. Wind-blown sand is one of the most destructive processes related to aeolian erosion [35]. This process can be considered as negligible for the western and northern entrances, but in the eastern one it is extremely decisive. The proximity of the sandy ground, the frequent high-speed wind prevailing in Nueva Tabarca Island, and the exposure of each façade to winds are the main factors controlling the intensity of the aeolian erosion.

The proximity of the sandy ground is a limiting factor due to the fact that short distances can be traveled by wind-blown particles. The grain diameter and the wind speed control the total grain distance. The distance of sand particles increases as the wind speed increases and the size decrease. Thus, the distance of a particle with a diameter of 0.25 mm and a velocity of 5 m/s is equal to 3.1 m [17]. The absence of loose particles in the surrounding northern and western entrances protects these doors from the wind-blown grains erosion. This is not the case of the eastern entrance, where the aeolian erosion is revealed as one of the most aggressive decay processes.

The exposure of a façade to the mean winds as well as to the extreme events is crucial for determining the susceptibility of this element to wind erosion. Figure 8 shows the orientation of the three studied city-wall doors to wind. Eastern entrance has an open exposure to the eastern winds, which prevails during the summer season. The other two entrances are preferentially exposed to the autumnal and wintry winds (W and WNW directions). The configuration of the city-walls around the northern and western entrances produces a shadow zone over the door, which stops part of the seasonal winds and reduces the effective zone (figure 8). Consequently, the northern entrance is strongly protected from the main wind directions, whilst the eastern entrance is the most expossed to the fast summer winds (figure 8). This fact emphasizes the aggressiveness of the wind abrasion action on the eastern entrance because it depends on the impact velocity of the wind-blown grains, and consequently, on the wind speed [17]. However, the abrasive capacity of the wind-blown particles does not increase linearly with wind speed [36]. Slight increments of the amount of eroded material occurs when wind speed increase up to 15 m/s [35]. At speed above 15 m/s, the aeolian abrasion and the mass loss grow exponentially.

Shi and Shi [17] concluded that the erosion damage caused by wind-blown sand has a stratification pattern that comprises three layers. The first one (the closest to the ground) show an increase of abrasive capacity from bottom to top. The second one is the saturation layer, where occurs the maximum abrasion. Finally, the aeolian abrasive capacity decrease in the third layer. In this profile, the maximum abrasion rate occurs at a certain height above the ground. Shi and Shi obtained the maximum point at 22 mm when wind speed is 0.51 m/s and the diameter of sand particles is 0.3 mm. This critical height shifts upward when wind velocity increase. This abrasive capacity profile agrees the erosion profile observed in the eastern entrance (figure 5) where a maximum recession depth is close to the ground level and decreases with the increment of height. In this case, the abrasive capacity profile is overlapped to the specific lithological map of the façade, and therefore, the mechanical resistance of stones nuances the potential erosion.

Table 1 shows the abrasion resistances obtained for the building stones used in the architectural heritage of Nueva Tabaraca island after the modified Böhme abrasion test. According to the mBAL values, the most resistant varieties are AA1 and C1 (211.75 and 214.02 mm^3, respectively) whilst the softest stones are AB3 and C2 (1204.77 and 1264.61 mm^3, respectively). This value is an indirect measurement of the resistance to the disintegration of superficial grains, and consequently, the softest varieties are the most sensitive ones to the aeolian abrasion, as well as to all the superficial decay processes acting at or just below the stone surface [36].

Besides the abrasion generated by the impact of wind-blown particles, wind is also related to other weathering processes, such as alveolization and wind-driven rain erosion. Although alveolization is not the most frequenty decay pattern in the three studied city-wall doors, some well-developed examples can be found, especially in the upper parts of the monuments and preferentially developed in the AB3 variety. Alveolization is related to the salt crystallization under windy conditions due to the evaporation of water from the porous system of the rock [15]. The fact that weathered stones are observed on the upper parts of the city-wall doors indicates that salt supply is carried out by sea-spray deposition [9, 11]. Once sea-spray has been deposited on the stone surface, it penetrates towards the inside of the stone. Then, wind-enhanced evaporation of the saline solution induces the formation of subefflorescence, resulting in granular disintegration and, eventually, in honeycomb formation [15]. This process will be more important in the AB3 variety, due to its low evaporation coefficient (E in table 1) and its low abrasion resistance (mBAL in table 1), which favor the apparition of subefforescences and superficial detachment, respectively.

Wind-driven rain (WDR) is defined as the rain with a horizontal velocity component given by the wind. Some authors consider WDR as one of the main factors being responsible for stone surface erosion, especially in rainy areas [18]. Driven drops impact on the rock surface and its deterioration action depends on the impact angle, the both wind and drop velocity and the drop size. Alicante region is classified as a “sheltered exposure” area due mainly to the very scarce rainfall [38]. As a consequence, the effects of WDR in the architectural heritage are expected to be very low. However, these results consider a daily database, and therefore, the intensity of the rainy event is not taken into account. The Nueva Tabarca climate, as well as Alicante region in general, has torrential rains during autumn and winter. Rainfall intensities higher than 20 mm/h were registered (24.3 mm/h on the 2nd of March of 2010 with winds of 11 m/s, and 32.1 mm/h on the 27th of January of 2011 with winds of 10 m/s). The maximum intensity of these heavy rainfalls had a brief duration (less than 30 minutes) but the total rainy event can extents up to 90 minutes with moderate-high intensity. Raindrop size distribution models for USA, Canada and UK confirms that heavy rain events having more than 10 mm/h rainfall intensity present reasonable portion of raindrops with 4 mm diameter [18]. Extreme rainfalls events are more intense and present bigger raindrop size, and consequently, it has strong erosive power than normal rains. WDR is not a dominant and continuous weathering process in Nueva Tabarca Island. However, its extremely high intensity and aggressiveness can contribute to explain the unpredictable, episodic and sometimes catastrophic stone breakdown [39].

3.5. Analysis of the representativeness of artificial ageing tests

The salt crystallization standard test [26] is the most common ageing test for assessing the rock durability and weathering resistance. This procedure is widespread used for predicting and modelling the building stone behaviour under natural conditions. Results from this test, as well as the direct measurements carried out on the monuments of Nueva Tabarca, have been used in this study for calculating the Equivalent Years parameter (Y_{eq}). This novel parameter quantifies the representativeness of the artificial ageing test. Y_{eq} accounts the number of years of natural ageing required for achieving the same weathered state of rocks after an artificial ageing test. This parameter (expressed in years) is calculated as (eq.3):

$$Y_{eq} = \frac{DWL/\rho_{bulk}}{S_{total}} \cdot \frac{t_{exp}}{MRD} \qquad \text{Eq. 3}$$

where: DWL (g) is the dry weight loss after 50 cycles of salt crystallization test (table 1); ρ_{bulk} (g/mm^3) is the bulk density (table 1); S_{total} (mm^2) is the total surface of the sample tested in laboratory, taking into account the six faces of the prismatic geometry; t_{exp} (years) is the exposure time of the stone blocks under the natural weathering conditions (in the case of Nueva Tabarca monuments, t_{exp} can take two values: 244 years for original ashlars and 39 years for replaced ashlars); and MRD (mm) is the mean recession depth measured in the stone bocks of the monument (table 2). The first part of the equation summarizes the weathering intensity of the rock samples at laboratory, whilst the second part of the equation expresses the real erosion of the rock in the monument.

Table 6 shows the Y_{eq} values for the rock varieties used in the studied city-wall doors. Hard (AA1, AB1 and C1) and soft rocks (AA2, AB3 and C2) present different values. For hard rocks, the weathering degree after the salt crystallization test is negligible and it agrees the good conservation state of these rocks in monuments. In these rocks, 50 cycles of artificial ageing are equivalent to rock exposures ranging between 0.1 and 4 years under real climatic conditions. For soft rocks, Y_{eq} values ranges widely from 20 to 165 years for original ashlars. In the eastern entrance, 50 salt crystallization cycles are equivalent to ~28 years of natural ageing, whilst in the northern entrance, Y_{eq} can achieve values up to 165 years.

Figure 9 shows the mathematical relationship between Y_{eq}, t_{exp}, DWL and MRD. Three theoretical situations are considered (t_{exp} = 40, 250 and 400 years). The solid lines drawn inside the graphs refer to different hypothetical conservation states of building stones in a monument (from fresh to intensely weathered: MRD=1mm, 10 mm, 50 mm, 100 mm and 200 mm). Areas marked in orange and grey delimit points with inconsistent information. On the one hand, orange areas represent the theoretical situation in which a building stone is classified as soft rocks after the artificial ageing tests but that shows good preservation state in the monument. On the other hand, grey areas mark the contrary hypothetical situation: rocks with negligible weight loss during the salt crystallization test at laboratory but moderate-intense erosion depths in the monuments. For example, red star in figure 9 represents a theoretical building rock which lost around 70% of its weight during the salt crystallization test (very low weathering resistance) but the erosion depth measured in monument is around 6 mm after 40 years of exposure to the local environment (moderate-high weathering resistance). On the contrary, blue star considers a rock with moderate-high weathering resistance after the artificial ageing test (~15% weight lost) but a high decay rate in monument (~30mm in only 40 years). Therefore, rocks plotted inside the orange areas correspond to building stones whose weathering resistance has been underestimated after the salt crystallization test, whilst the points included in the grey areas represent rocks overestimated.

Discrepancies between artificial and natural ageing processes can be explained considering (1) differences between the controlled conditions established for laboratory tests and the natural decay mechanisms acting in real situations; and (2) the aggressiveness degree of the environment surrounding the monument. On the one hand, in our case, mirabilite crystallization process is much more aggressive than halite crystallization and, consequently, samples in laboratory trend to be much more decayed than in real conditions (for further explanation, see [15,30]). Soft rocks are much more sensitive to this effect and, consequently, AA2 and especially AB3 and C2, trend to present artificial ageing rates higher than those observed under real environments. In some case, rock resistance to decay can result highly underestimated by the salt crystallization test (C2/N-SM and AB3/N-SM in figure 9). On the other hand, the lowest values of Y_{eq} in the original ashlars of soft rocks (AA2, AB3 and C2) are obtained in the eastern entrance (table 6 and figure 9). This is due to the high aggressiveness of the environment surrounding this city-wall door. The eastern entrance registered the worst ageing conditions because had the lowest relative humidity (the lowest of the three studied environments). This causes a higher number of salt transitions and a more effective crystallization pressures related to longer periods of low relative humidity. Moreover, the preferential exposure of this façade to wind and especially to wind-blown particles during the summer, accelerate the stone erosion. The northern and western entrances present higher relative humidities and, moreover, the northern entrance is strongly protected from the main wind directions. The high environmental aggressiveness is translated in low Y_{eq} because of the fact that the real erosion depth (MRD in the previous equation) is higher than the dry weight loss (DWL) obtained in laboratory.

An open discussion exists about how representative the artificial ageing tests are in relation to the natural ageing. One of the main problems is the fact that stone decay is a dynamic process and evolves into an inherently complex system, in which processes evolution and rates may change due to many factors both intrinsic and extrinsic to the material. Most standardized accelerated stone decay tests are based on the assumption that decay will occur always linearly and that an indicator based on the comparison between the final and the initial values of certain parameter will give a result proportional to the durability of certain stone type that can serve as comparison to other stone types. However, stone decay behaves most often as a non-linear system [40].

Non-linear decay pattern is observed in the studied building stones. Erosion depths are much lower in the rebuilt parts of the monuments than they are in the original ashlars. That fact is reflected in the lower Y_{eq} values of the replaced stones (table 6). Several intrinsic factors help to understand, in general terms, the non-linear decay of building stones. For example, anisotropy of the weathering process, energy decrease from crack formation to crack propagation and pore form and size variations throughout the decay process [41]. However, the exceptional nature of some external factors (such as wind-driven rain or wind-blown particle erosion) enhances the non-linear erosion of stone surface. For example, heavy rainfalls have a washing effect, removing detached particles or weak parts of stone previously decayed by other processes such as salt crystallization. The longer the exposure period, the more weakened the stone surface, and consequently, the higher the erosive capacity of the punctual extreme events.

Finally, artificial ageing tests represent simplified weathering systems in which a limited number of variables play in a way exceptionally aggressive on the rock during a brief period of time. Real conditions differ from this controlled system in several points: i) the aggressiveness, the repeatability and the recurrence of the cycles is lower; ii)weathering agents act during longer exposure periods; and iii) do not exist a limited number of variables acting in the natural weathering process and, consequently, multiple decay processes can act simultaneously and subsequently. In this paper, several essential factors controlling the rock weathering have been analysed. However, others processes remain untreated, such as clay swelling, chemical dissolution of calcite, halite damage by thermal expansion as well as the effects of biological factors. All these factors can have significant effects on rock weathering under marine environments [12,22] and they will be treated in future works, contributing to the better understanding of the stone weathering of Nueva Tabarca fortress.

4. Conclusions

Six different rock varieties were identified in the three studied city-wall doors of Nueva Tabarca fortress: AA1, AA2, AB1, AB3, C1 and C2. AB3 is the softest variety mainly due to its pore-size distribution (one main pore population centered between 0.2 and 1 µm) and low mechanical resistance (strength around 24.34 MPa after the Point Load Test and mBAL values around 1204.77 mm^3 after the modified Böhme Abrasion Test). Consequently, this variety shows high weight loss during the salt crystallization test (DWL~78.59%) and it agrees with the erosion rates measured in this rock in the monuments. On the other hand, AB1, C1 and AA1 present the highest values in the mechanical paramenters and they have a wide pore-size distribution. As a consequence, they are the more resistant rock varieties. The Böhme abrasion test proposed in this paper has successfully been used for assessing the superficial resistance of rocks to the erosion by wind-blown particles.

Nueva Tabarca climate showed a significant increase in the frequency of halite crystallization-dissolution transitions at the end of autumn (November-December) and during winter (January-February). This increase is not only registered in the number of salt transitions but also in the duration of the periods in which the relative humidity is continuously under the critical values (RH=75.3% and RH=63.5%). Measurements of the microclimatic variables at the specific environment surrounding the three studied city-wall doors show that eastern city-wall door is the dryest. The relative humidity in this point is between 5 and 23% lower than it is in the other two entrances. As a consequence, specific salt transitions in the eastern entrance are expected to be more frequents and more prolonged than they are in the northern and western entrances.

Two preferential wind directions are registered along the year. Eastern winds prevailed during summer (from May to September), whilst W and WNW directions were preferentially registered from the end of autumn (November) to February. Wind is revealed as an important erosion agent in Nueva Tabarca fortress due to its capacity for the wind-blown particles abrasion and its contribution to the formation of subefflorescences in rocks. Moreover, despite the fact that the rainfall in the Mediterranean semiarid climate is very scarce, the wind-driven rain is here an important mechanism for removing detached particles from weathered rock surfaces due to its torrential characteristics.

The eastern city-wall door is the most decayed entrance (mean recession depth of 68 mm). Erosion intensity depends strongly on the building rock varieties used in each monument, being preferentially used AB3 and AB1 in the eastern entrance, and AA2, AB1 and C1 in the other two city-wall doors. The use of the softest rock varieties in the eastern entrance is worsened by the high aggressiveness of its surrounding microclimatic conditions. In addition to the dry conditions registered in this entrance, this façade presents a preferential exposure to eastern winds. The northern and western entrances present higher relative humidities and the northern entrance, particularly, is strongly protected from the main wind directions.

Two different vertical erosion profiles are defined in the studied façades. On the one hand, the eastern city-wall door has down area intensely decayed and an upper part slightly eroded. On the other hand, the erosion pattern is different in the other two entrances, where the upper area results much more weathered than the bottom part. The aeolian abrasion causes preferential erosion of the down parts of the eastern city-wall door. This erosion mechanism is especially effective during extreme events in summer, where the high energy eastern winds move the loose particles of the surrounding sandy ground. On the contrary, the preferential erosion of the upper parts of the city-wall doors is related to the wind-enhanced evaporation of the saline solution supplied by sea-spray deposition. These processes are more important in the northern and western entrances due to the proximity to the coastline. Moreover, AB3 is especially sensitive to this process due to its highest content of micropores and its low both evaporation coefficients and mechanical properties.

Finally, results obtained with the new parameter Equivalent Years (Y_{eq}) conclude that durability of soft rocks (AA2, and especially AB3 and C2) is underestimated by the artificial ageing tests (salt crystallization test), especially when short laboratory tests are compared with long natural exposure periods. A wide range of Y_{eq} values are obtained for these rocks (from 8 to 165 years), showing a strong dependency with both the exposure time as well as the agressiveness of the exposing environment. In the case of AA1, AB1 and C1 (the hardest rocks studied in this paper), their low weathering degree achieved during the standardized salt crystallization test is equivalent to exposure times ranging from 0.1 to 4 years under real climatic conditions, being values much lower than those obtained for soft rocks.

Acknowledgements

The authors wish to thank José Manuel Pérez Burgos, Felio Lozano and Antonio Ruso for their disinterested collaboration during the data collection and field works. This research was supported by project GRE12-03 (University of Alicante).

References:

[1] Barone, G., Mazzoleni, P., Pappalardo, G., Raneri, S. (2015): Microtextural and microstructural influence on the changes of physical and mechanical properties related to salts crystallization weathering in natural building stones. The example of Sabucina stone (Sicily). Construction and Building Materials, 95: 355-365.

[2] Andriani, G., & Walsh, N. (2003). Fabric, porosity and water permeability of calcarenites from Apulia (SE Italy) used as building and ornamental stone.*Bulletin of Engineering Geology and the Environment*, *62*(1), 77-84.

[3] Gaied, M.E., Gallala, W., Younés, A. (2015): Geoarcheology of Roman Underground Quarries at Ksour Essaf (Tunisia). Geoheritage, 7: 375-382.

[4] Cassar, J. (2002): Deterioration of the Globigerina limestone of the Maltese Islands. In: Natural stone, weathering phenomena, conservation strategies and case studies. Siegesmund, S., Weiss, T., Vollbrecht, A. (Eds). Geological Society, London, Special Publication, 205: 33-49.

[5] Genestar, C., Pons, C., Cerro, J.C., Cerà, V. (2014): Different decay patterns observed in a nineteen-century building (Palma, Spain). Environ Sci Pollut Res, 21: 8663-8672.

[6] Mateos, R.M., Durán, J.J., Robledo, P.A. (2011): Marès Quarries on the Majorcan Coast (Spain) as Geological Heritage Sites. Geoheritage, 3: 41-54.

[7] Louis, M., García del Cura, M.A., Spairani, Y., de Blas, D. (2001): The Civil Palaces in Gravina Street, Alicante: building stones and salt weathering. Materiales de Construcción, 51: 23-37.

[8] Colston, B. J., Watt, D. S., & Munro, H. L. (2001). Environmentally-induced stone decay: the cumulative effects of crystallization–hydration cycles on a Lincolnshire oopelsparite limestone. *Journal of cultural heritage*, *2*(4), 297-307.

[9] Cardell, C., Delalieux, F., Roumpopoulos, K., Moropoulou, A., Auger, F., Van Grieken, R. (2003). Salt-induced decay in calcareous stone monuments and buildings in a marine environment in SW France. *Construction and building materials*, *17*(3), 165-179.

[10] Andriani, G.F., Walsh, N. (2007). The effects of wetting and drying, and marine salt crystallization on calcarenite rocks used as building material in historic monuments. *Geological society, London, special publications*, *271*(1), 179-188.

[11] Stefanis, N.A., Theoulakis, P., Pilinis, C. (2009): Dry deposition effect of marine aerosol to the building stone of the medieval city of Rhodes, Greece. Building and Environment, 44: 260-270.

[12] Benavente, D., Sanchez-Moral, S., Cortes-Fernández, A., Cañaveras, J.C., Elez, J., Saiz-Jiménez, C. (2011): Salt damage and microclimate in the Postumius Tomb, Roman Necropolis of Carmona, Spain. Environmental Earth Sciences, 63: 1529-1543.

[13] Bellopede, R., Catelletto, E., Marini, P. (2016): Ten years of natural ageing of calcareous stones. Engineering Geology, 211: 19-26.

[14] Ruedrich, J., Seidel, M., Rothert, E., Siegesmund, S. (2007): Length changes of sandstones caused by salt crystallization. From: Prikryl, R., Smith, B.J. (eds). Building stone Decay: from Diagnosis to Conservation. Geological Society, London, 272: 199-209.

[15] Rodriguez-Navarro, C., Doehne, E., Sebastián, E. (1999): Origins of honeycomb weathering: The role of salts and wind. GSA Bulletin, 111.

[16] Gomez-Heras, M., Fort, R. (2007): Patterns of halite (NaCl) crystallisation in building Stone conditioned by laboratory heating regimes. Environmental Geology, 52: 259-267.

[17] Shi, X.J., Shi, X.F. (2014): Numerical prediction on erosion damage caused by wind-blown sand movement. European Journal of Environemtnal and Civil Engineering, 18: 550-566.

[18] Erkal, A., D'Ayala, D., Sequeira, L. (2012): Assessment of wind-driven rain impact, related surface erosion and surface strength reduction of historic building materials. Building and Environment, 57: 336-348.

[19] Beviá, M., Giner Martínez, J. (2012): Nunc Minerva postea Palas: la ciudad de Nueva Tabarca. Canelobre, 60: 114-127 (in Spanish).

[20] ICOMOS-ISCS (2008): Illustrated glossary on stone deterioration patterns. http://international.icomos.org/publications/monuments_and_sites/15/pdf/Monuments_and_Sites_15_ISCS_Glossary_Stone.pdf

[21] Bromblet, P. (1994): Les techniques d'analyse appliquées à l'ètude des alterations de la pierre des monuments. Bulletin de l'Association des conservateurs des antiquités et objets d'art de France: 21-33.

[22] Mottershead, D., Gorbushina, A., Lucas, G., Wright, J. (2003): The influence of marine salts, aspect and microbes in the weathering of sandstone in two historic structures. Building and Environment, 38: 1193-1204.

[23] UNE-EN 14157 (2005). Natural Stone test methods. Determination of the abrasion resistance. AENOR –CEN, 21 pp.

[24] UNE-EN 1925 (1999). Natural stone test methods. Determination of water absorption coefficient by capillarity. AENOR –CEN, 14 pp.

[25] ASTM D5731-95: Standard Test Method for Determination of the Point Load Strength Index of Rock. ASTM International, West Conshohocken, PA.

[26] UNE-EN 12370 (1999): Métodos de ensayo para piedra natural. Determinación de la resistencia a la cristalización de sales. AENOR –CEN, 12 pp.

[27] Steiger, M., Charola, A.E., Sterflinger, K. (2011): Weathering and deterioration. In: *Stone in architecture*. Springer Berlin Heidelberg: 227-316.

[28] Siegesmund, S., Dürrast, H. (2011): Physical and mechanical properties of rocks. In: Stone in Architecture. Siegesmund, S. and Snethlage, R. (Eds.). Springer-Verlag, Berlin.

[29] Snethlage, R. (2005): Leitfaden Steinkonservierung (Guideline for stone conservation), 2nd revised edn., IRB, Stuttgart

[30] Benavente, D., Brimblecombe, P., Grossi, C.M. (2015): Termodynamic calculations for the salt crystallisation damage in porous built heritage using PHREEQC. Environ Earth Sci, 74: 2297-2313

[31] Grossi, C.M., Brimblecombe, P., Menéndez, B., Benavente, D., Harris, I., Déqué, M. (2011): Climatology of salt transitions and implications for stone weathering. Science of the Total Environment, 409: 2577-2585.

[32] Price, C. (1978). The use of the sodium sulphate crystallization test for determining the weathering resistance of untreated stone. Deterioration and Protection of Stone Monuments. International Sysmposium, Paris, 3.6. 10 pp.

[33] Sillmann, J., Kharin, V.V., Zwiers, F.W., Zhang, X., Bronaugh, D. (2013): Climate extremes indices in the CMIP5 multimodel ensemble: part 2. Future climate projections. Journal of Geophysic Research: Atmosphera, 118, 2473-2493.

[34] Pla, C., Cuezva, S., Garcia-Anton, E., Fernandez-Cortes, A., Cañaveras, J.C., Sanchez-Moral, S., Benavente, D. (2016): Changes in the CO2 dynamics in near-surface cavities under a future warming scenario: Factors and evidence from the field and experimental findings. Science of the Total Environment, 565: 1151-1164.

[35] Zhao, D., Lu, W., Wang, Y., Mao, X., Ai, Y., Jiang, H. (2016): Experimental Studies on Earthen Architecture Sites Consolidated with BS Materials in Arid Regions. Advances in Materials Science and Engineering, 2016: 13 pp.

[36] Camuffo, D. (1995): Physical weathering of stones. The Science of the Total Environment, 167:1-14.

[37] Vergès-Belmin, V. (2010): Deterioration of Stone in Monuments. In: Environmental Geomechanics. Schrefler, B. and Delage, P. (Eds). ISTE Ltd, London (UK).

[38] Pérez-Bella, J.M., Domínguez-Hernández, J., Rodríguez-Soria, B., del Coz-Díaz, J.J., Cano-Suñén, E. (2012): Estimation of the exposure of buildings to driving rain in Spain from daily wind and rain data. Building and Environment, 57: 259-270.

[39] Smith, B.J., Gomez-Heras, M., Viles, H.A. (2010): Underlying issues on the selection, use and conservation of building limestone. London: Geological Society, Special Publication, 331; p.1-11.

[40] Viles, H.A. (2005): Can stone decay be chaotic? In: Turkington AV, editor. Stone decay in the architectural environment, Boulder (Colorado): Geological Society of America, Special Publication 390; p.1-11.

[41] Martínez-Martínez, J., Benavente, J., Gómez-Heras, M., Marco-Castaño, L., García-del-Cura,M.A. (2013): Non-linear decay of building Stones Turing freeze-thaw weathering processes. Const. Build. Mat, 38: 443-454.

Figure captions:

Figure 1: Top: Nueva Tabarca island location. Center: plan of the Nueva Tabarca fort with location of the historic quarries and the three city-wall entrances. Down: photographies of the three studied city-wall doors showing both the current state and the conservation state previously to the rebuilding works of 1975.

Figure 2: Optical photomicrographs (parallel polarised light) of studied rock varieties.

Figure 3: Pore size distribution of the studied rocks (MIP method).

Figure 4: Fresh and artificially weathered samples (salt crystallization test at laboratory).

Figure 5: lithology and erosion maps of the three studied city-wall doors. Areas delimited in red correspond to rebuilt parts.

Figure 6: weathering forms observed in the rock ashlars of Nueva Tabarca fort. (a) differential erosion in AA2 variety with laminated structure. (b) Deep alveolization in AB3. (c) rounded ashlar of AB1. (d) and (e) (detail) differential erosion developed in C2 where fossil components (rhodoliths) result in relief. (f) scaling developed in AB1.

Figure 7: RH-T data registered during the study period.

Figure 8: Wind directions and wind exposure of the three studied city-wall doors. Wind direction is expressed in two different ranges: monthly mean direction considering all the windy episodes (independently of its velocity) (showed in black) and the mean direction of the monthly extreme events (windy episodes with wind speed higher than 10 m/s) (showed in red). E-SR: East entrance (San Rafael); N-SM: North entrance (San Miguel); W-SG: West entrance (San Gabriel).

Figure 9: Graphical relationship between Y_{eq}, t_{exp}, DWL and MRD. *Note: the presented correlation between DWL (in %) and $DWL/\rho/S_{TOT}$ (in mm) is only valid when 40x40x40mm cubic samples are considered.

Table 1. Porous system characterization and hydro-mechanic properties of studied rocks. Decay forms: rounding, R; sanding, S; cracking, C; differential erosion in laminated structures, DE_{lam}, and differential erosion eliminating the rock matrix, DE_m. In brackets: cycle in which the decay form appears for the first time.

	AA1	**AA2**	**AB1**	**AB3**	**C1**	**C2**
Porous system characterization						
ρ_{bulk} [g/cm3]	2.08	2.05	2.07	2.34	2.17	2.12
ϕ_o [%]	21.78	24.13	21.65	16.15	19.97	20.30
ϕ_{cap} [%]	18.49	18.93	17.18	13.11	17.02	18.26
ϕ_{Hg} [%]	22.28	19.86	23.90	15.13	18.30	24.09
r_M [µm]	0.37	0.10	0.21	0.10	0.17	0.26
r_{MD} [µm]	2.41	1.08	2.76	0.59	1.97	0.57
Hydric properties						
C [$Kg/m^2h^{0.5}$]	5.04	9.01	8.01	2.88	11.65	4.67
E [$Kg/m^2h^{0.5}$]	3.38	3.89	4.42	1.80	3.47	2.55
Mechanical properties						
PLT [MPa]	45.73	34.84	36.37	24.34	65.66	45.61
mBAL [mm^3]	211.75	353.22	376.38	1204.77	214.02	1264.61
Durability						
DWL [%]	0.16	23.43	0.11	78.59	0.54	20.53
Decay forms	-	S(5) DE_{lam}	R(10)	S(3) C(4)	R(15)	S(7) DE_m

Table 2: Mean recession depths (MRD, in mm) in the three studied city-wall doors. E-SR: East entrance (San Rafael); N-SM: North entrance (San Miguel); W-SG: West entrance (San Gabriel).

	Original stones			Replacement stones		
	E-SR	**N-SM**	**W-SG**	**E-SR**	**N-SM**	**W-SG**
AA1	[-]	20.00	1.67	1.70	5.40	8.30
AA2	35.87	31.67	14.08	[-]	[-]	[-]
AB1	18.93	29.38	10.28	4.90	18.75	15.00
AB3	168.95	37.13	[-]	67.50	23.44	51.58
C1	[-]	15.80	6.25	[-]	10.00	2.50
C2	22.50	5.00	[-]	2.50	[-]	[-]
min	0.30	0.48	0.00	0.00	2.07	0.00
mean	68.54	24.08	9.00	8.60	16.34	36.60
max	275.18	161.02	66.34	67.05	33.82	66.35

Table 3: Climatic data of Nueva Tabarca island. Non available data in January 2010 and April-Jun 2010.

		temperature [ºC]		RH [%]		Rainfall	Transitions for NaCl					
							[RH<75.3%]			[RH<63.5%]		
	days	mean	[min-max]	mean	[min-max]	[mm]	^{75}T	$^{75}T_{0.5}$ ($^{75}T_5$)	h	^{63}T	$^{63}T_{0.5}$ ($^{63}T_5$)	h
2009												
Apr	7	16.9	[13.0 - 21.2]	74.0	[37 - 94]	0.0	2	14 (7)	77.5	1	12 (4)	34.5
May	31	19.3	[13.7 - 23.2]	81.9	[41 - 95]	3.2	3	10 (4)	121.0	0	8 (3)	26.0
Jun	30	23.2	[18.3 - 29.8]	80.1	[36 - 94]	0.0	3	8 (6)	113.5	0	7 (4)	46.0
Jul	23	26.1	[22.8 - 31.6]	81.9	[48 - 94]	0.2	1	5 (3)	63.5	1	4 (1)	20.0
Aug	31	26.8	[23.4 - 30.2]	78.3	[50 - 90]	4.2	3	11 (5)	180.0	0	9 (2)	25.5
Sep	8	26.6	[24.7 - 30.4]	78.5	[54 - 90]	0.0	1	2 (0)	35.5	0	1 (0)	3.0
Oct	19	21.0	[16.8 - 24.9]	72.9	[38 - 93]	4.6	4	7 (5)	183.0	1	6 (4)	72.5
Nov	30	17.9	[10.3 - 26.6]	70.5	[32 - 92]	3.6	4	15 (11)	357.5	3	14 (8)	245.5
Dec	5	15.2	[11.6 - 19.2]	60.8	[39 - 81]	0.4	1	5 (4)	93.0	1	5 (3)	68.0
2010												
Feb	23	12.6	[5.5 - 21.1]	74.9	[32 - 95]	67.5	4	17 (7)	212.5	2	15 (6)	123.0
Mar	31	13.0	[6.0 - 21.1]	78.9	[35 - 97]	74.6	4	15 (8)	209.5	2	12 (6)	90.5
Jul	8	26.5	[24.7 - 29.6]	73.9	[59 - 88]	0.0	2	4 (0)	104.5	0	4 (0)	8.0
Aug	31	26.4	[22.4 - 32.9]	78.7	[40 - 95]	18.2	3	9 (4)	174.5	0	7 (2)	20.0
Sep	15	25.0	[22.2 - 31.1]	71.5	[38 - 86]	0.0	1	12 (4)	209.5	1	10 (3)	60.0
Oct	10	18.2	[12.1 - 23.3]	68.5	[30 - 87]	0.0	2	12 (6)	235.0	1	10 (4)	72.0
Nov	30	15.6	[9.4 - 23.4]	69.0	[36 - 94]	18.2	4	22 (15)	455.0	5	21 (13)	268.0
Dec	31	12.3	[3.6 - 19.3]	75.0	[34 - 94]	11.0	5	23 (9)	288.5	3	21 (7)	179.5
2011												
Jan	31	12.5	[4.3 - 20.2]	78.0	[36 - 96]	45.8	4	15 (5)	249.5	2	12 (5)	73.5
Feb	3	10.9	[7.4 - 15.2]	64.0	[48 - 78]	0.0	0	7 (3)	58.5	1	7 (3)	25.0

Table 4: micro-climatic conditions measured in the three city-wall entrances. E-SR: East entrance (San Rafael); N-SM: North entrance (San Miguel); W-SG: West entrance (San Gabriel).

	E-SR		**N-SM**		**W-SG**	
Day - Hour	T [ºC]	RH [%]	T [ºC]	RH [%]	T [ºC]	RH [%]
18 Dec – 16:00	17.78	65.00	14.79	77.3	15.72	72.40
15 Jan - 12:00	16.85	57.44	15.58	64.03	14.60	71.54
23 Jan - 12:00	13.31	54.4	12.35	60.57	13.10	57.75
23 Jan - 17:00	14.60	60.94	13.97	67.94	13.77	66.91
23 Jan - 19:30	13.24	66.45	12.61	71.10	13.40	69.2
24 Jan – 1:30	11.22	53.97	11.35	58.77	11.22	60.10
24 Jan – 16:30	17.56	36.01	17.31	42.23	17.55	39.75
02 Apr – 13:30	16.40	75.20	16.52	85.37	16.70	84.60
04 Apr – 20:00	21.82	21.90	20.60	32.90	19.95	38.50
28 Jul - 12:00	27.2	78.7	26.60	85.3	26.9	80.3
04 Aug -15:00	41.50	26.41	29.50	47.10	30.90	49.62

Table 5: wind direction and wind speed in Nueva Tabarca island. Non available data in January 2010 and April- Jun 2010.

			extreme events							
	mean Speed [m/s]	**mean direction** [º]	**>7.5 m/s**		**>10 m/s**		**>15 m/s**		**>20 m/s**	
			mean direction	hours	mean direction	hours	mean direction	hours	mean direction	hours
apr-09	6.4	236.5	203	43	201.6	24.5	202.5	9.5	202.5	1.5
may-09	4.7	69.7	75.9	105.5	135.4	20	64.6	1.5		0
jun-09	4.8	148.4	178.1	106	183.9	49	198.2	13		0
jul-09	4.9	97.1	75.7	76	54.1	26.5	45	9.5	45	3
aug-09	4.4	58.7	55	90.5	55.2	34	46.7	13	45	1.5
sep-09	6.4	78.1	62.8	53.5	64.2	10.5		0		0
oct-09	4.8	218.4	207.3	96	228.9	25	250.7	9		0
nov-09	5.4	269.9	272.5	37.5	262.9	2	337.5	0.5	370.5	0
dec-09	8.0	289	298.3	50	291	16.5		0		0
feb-10	5.7	277.6	285.9	130.5	207.4	40	209.4	7.5		0
mar-10	5.4	337.4	57.3	157.5	55.8	63	45	15	45	2.5
jul-10	2.9	111.9	112.3	0	112.3	0	112.3	0	112.3	0
aug-10	5.0	94.6	79.8	129.5	57.2	29.5	123.7	3		0
sep-10	4.4	82	185.4	27.5	200.7	6	202.5	0.5		0
oct-10	5.0	241.9	230.9	42	206.4	8.5	211.5	2.5		0
nov-10	5.9	280.6	272.6	167.5	222.6	41	219.4	8		0
dec-10	4.8	291.6	292.6	119.5	352.5	23	315	1	315	0.5
jan-11	5.0	296.7	40.7	132.5	39.6	54	45	8		0
feb-11	4.7	275.5	205.7	3.5		0		0		0

Table 6: Y_{eq} (in years) obtained for the rock varieties used in the studied city-wall doors. E-SR: East entrance (San Rafael); N-SM: North entrance (San Miguel); W-SG: West entrance (San Gabriel).

	Y_{eq} (years) in original ashlars		
	E-SR	N-SM	W-SG
AA1	[-]	0.33	3.90
AA2	28.55	52.33	72.73
AB1	0.24	0.16	0.45
AB3	19.26	87.64	[-]
C1	[-]	1.34	3.40
C2	36.85	165.81	[-]
	Y_{eq} (years) in replaced ashlars		
	E-SR	N-SM	W-SG
AA1	0.61	0.19	0.13
AA2	[-]	[-]	[-]
AB1	0.15	0.04	0.05
AB3	7.71	22.19	10.08
C1	[-]	0.34	1.36
C2	53.01	[-]	[-]

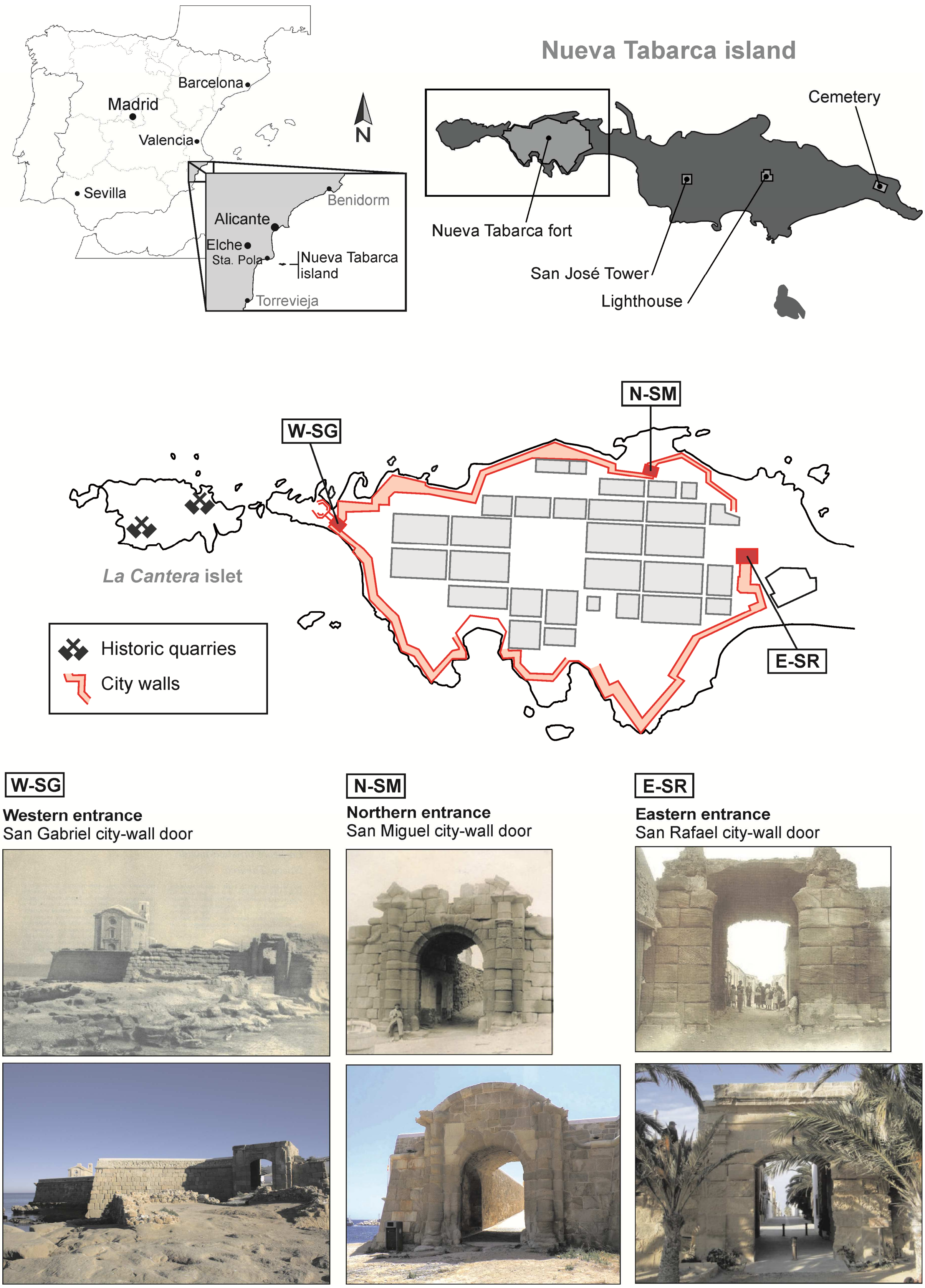
Nueva Tabarca island
Barcelona
Madrid
Valencia
Sevilla
N
Benidorm
Alicante
Elche
Sta. Pola
Nueva Tabarca island
Torrevieja
Cemetery
Nueva Tabarca fort
San José Tower
Lighthouse
N-SM
W-SG
La Cantera islet
Historic quarries
City walls
E-SR
W-SG
Western entrance
San Gabriel city-wall door
N-SM
Northern entrance
San Miguel city-wall door
E-SR
Eastern entrance
San Rafael city-wall door

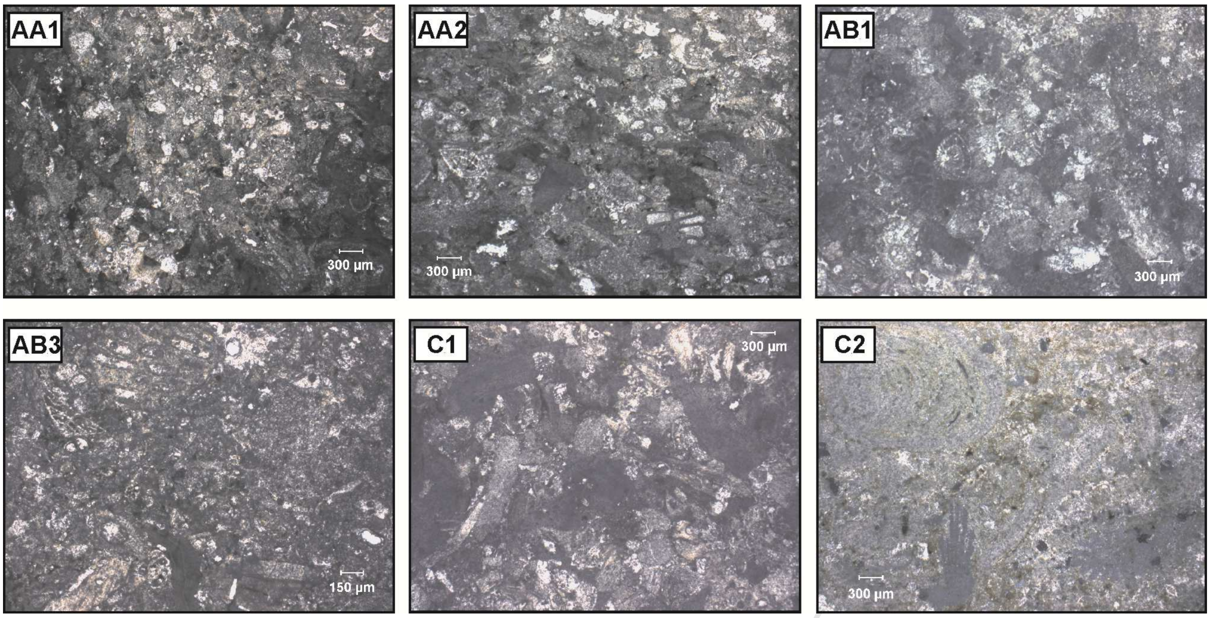
AA1
300 µm
AA2
300 µm
AB1
300 µm
AB3
150 µm
C1
300 µm
C2
300 µm

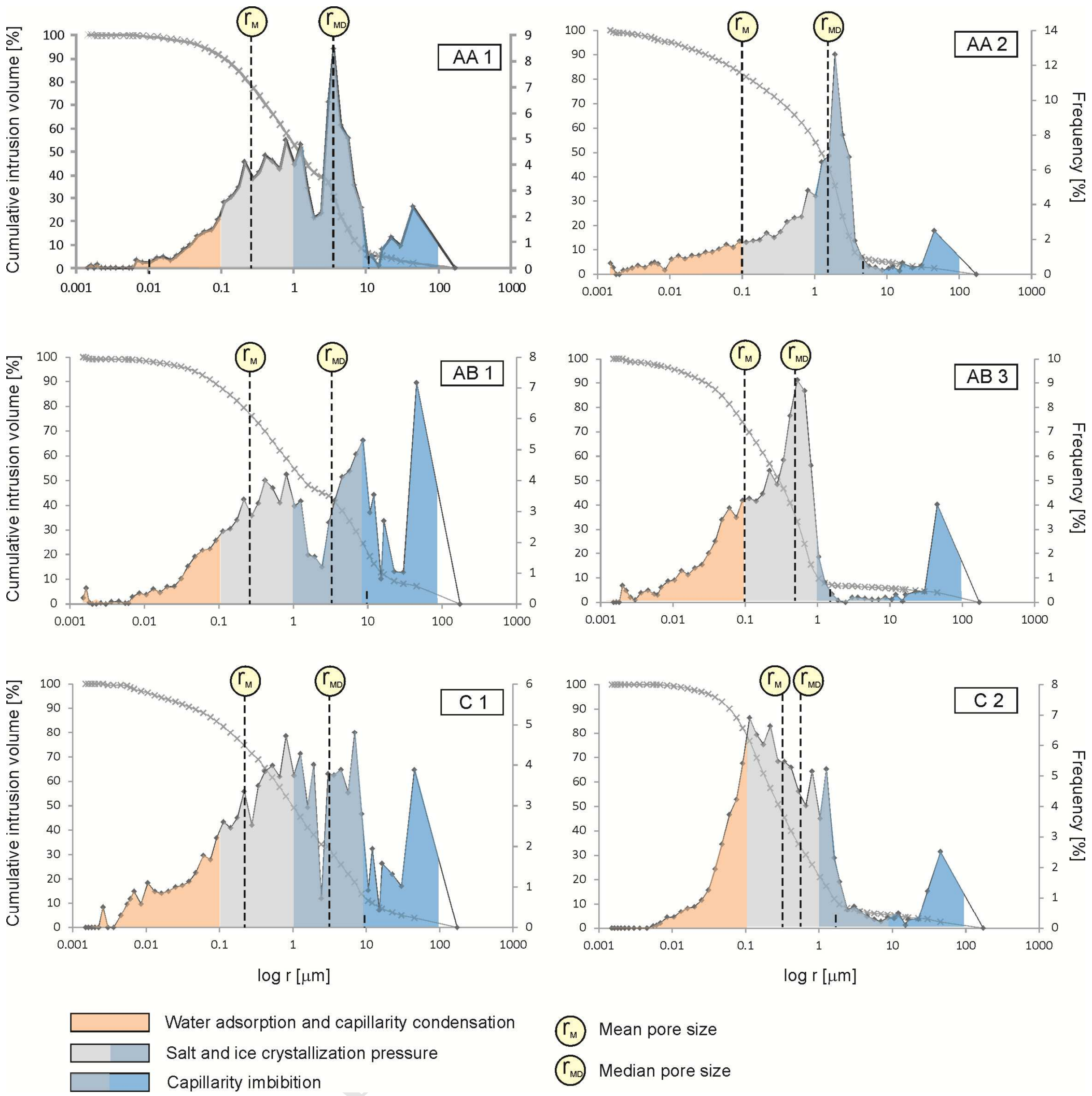

AA 1
AA 2
AB 1
AB 3
C 1
C 2
Cumulative intrusion volume [%]
Frequency [%]
log r [μm]
Water adsorption and capillarity condensation
Salt and ice crystallization pressure
Capillarity imbibition
Mean pore size
Median pore size


AB1
C2
AA2
AB3

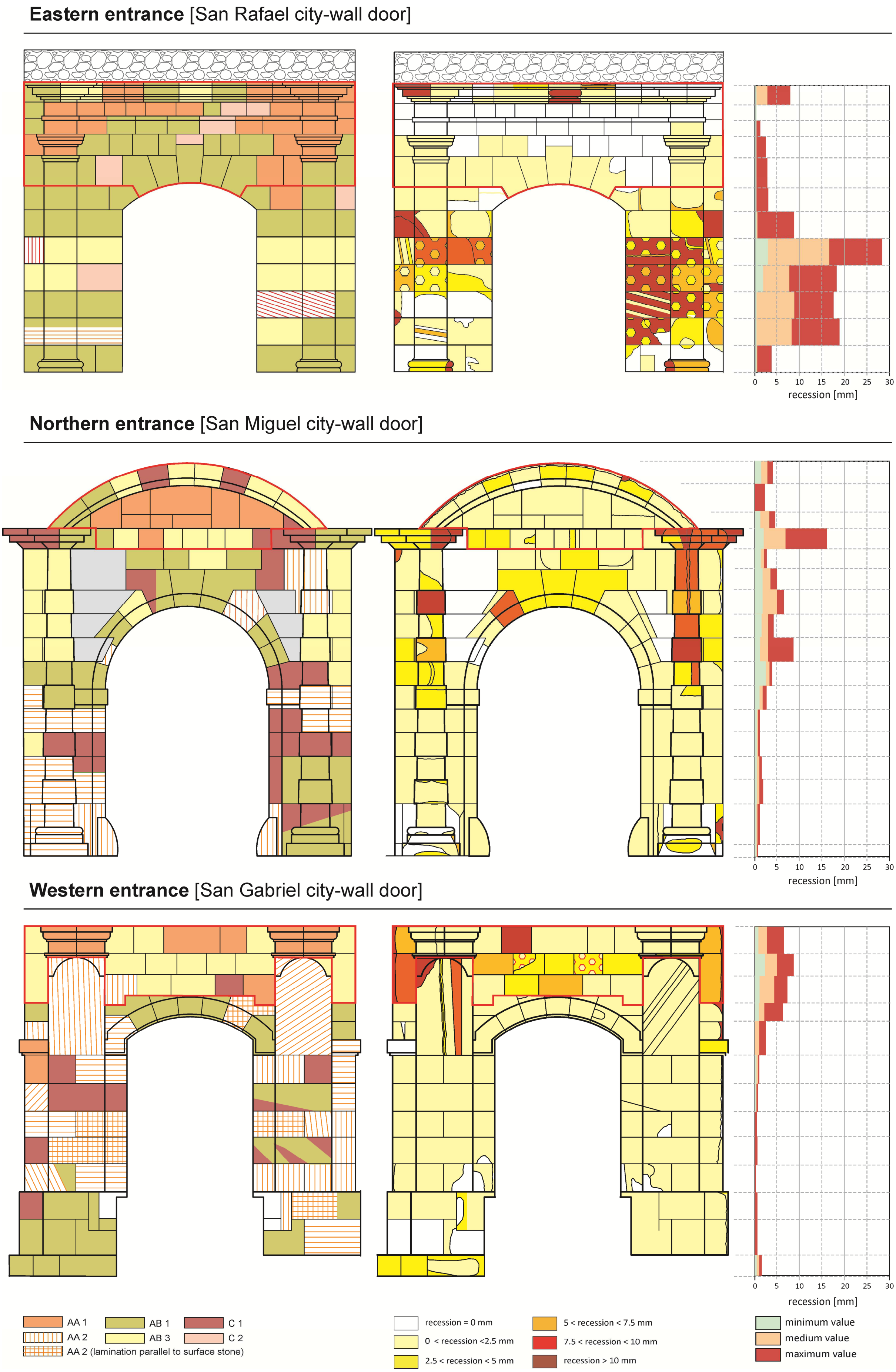

Eastern entrance [San Rafael city-wall door]
0 5 10 15 20 25 30
recession [mm]
Northern entrance [San Miguel city-wall door]
0 5 10 15 20 25 30
recession [mm]
Western entrance [San Gabriel city-wall door]
0 5 10 15 20 25 30
recession [mm]
AA 1
AA 2
AA 2 (lamination parallel to surface stone)
AB 1
AB 3
C 1
C 2
recession = 0 mm
0 < recession <2.5 mm
2.5 < recession < 5 mm
5 < recession < 7.5 mm
7.5 < recession < 10 mm
recession > 10 mm
minimum value
medium value
maximum value

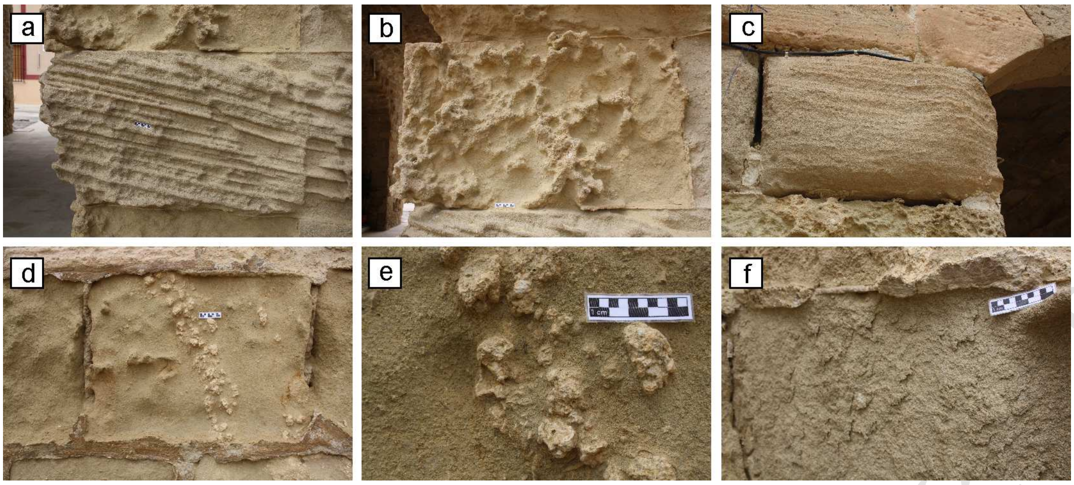
a
b
c
d
e
1 cm
f

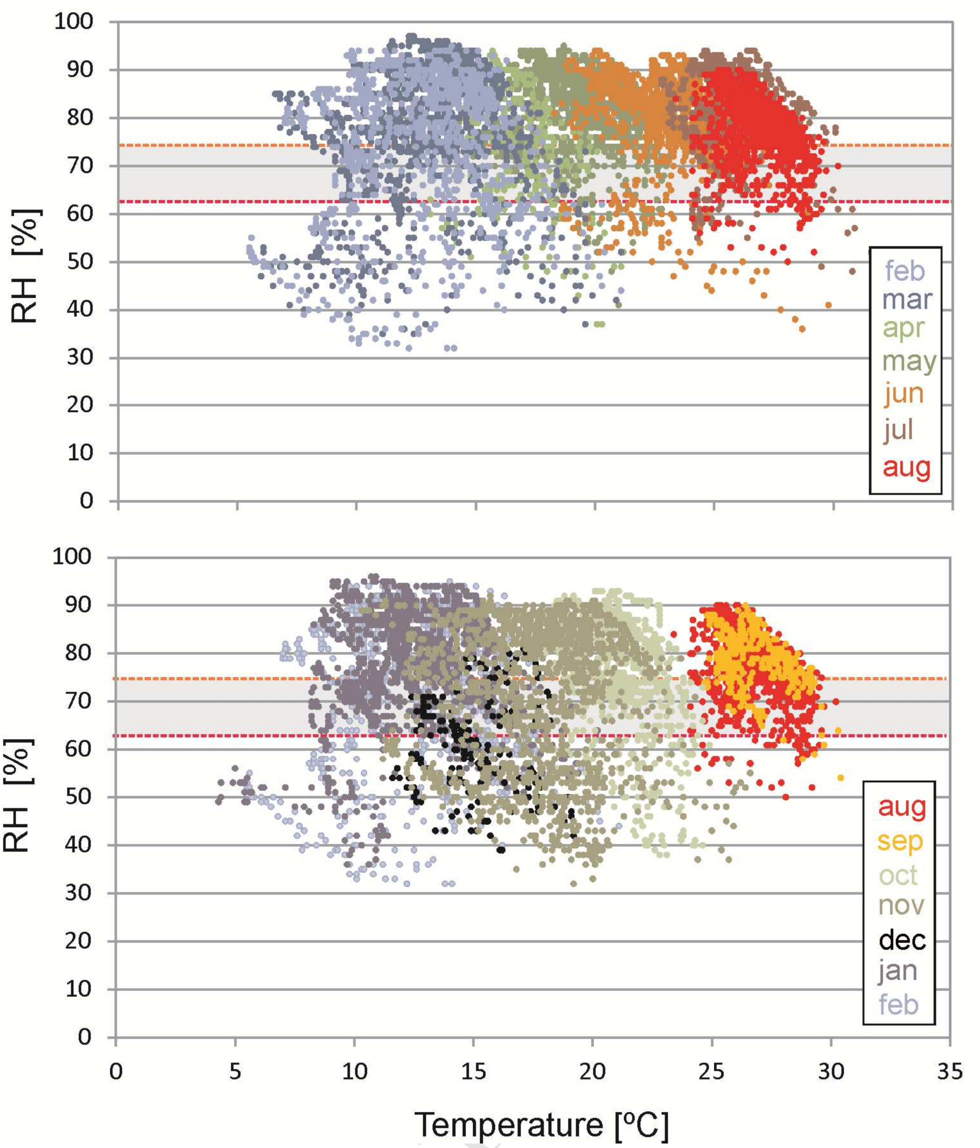
100
90
80
70
60
50
40
30
20
10
0
RH [%]
feb
mar
apr
may
jun
jul
aug
RH [%]
aug
sep
oct
nov
dec
jan
feb
0
5
10
15
20
25
30
35
Temperature [ºC]

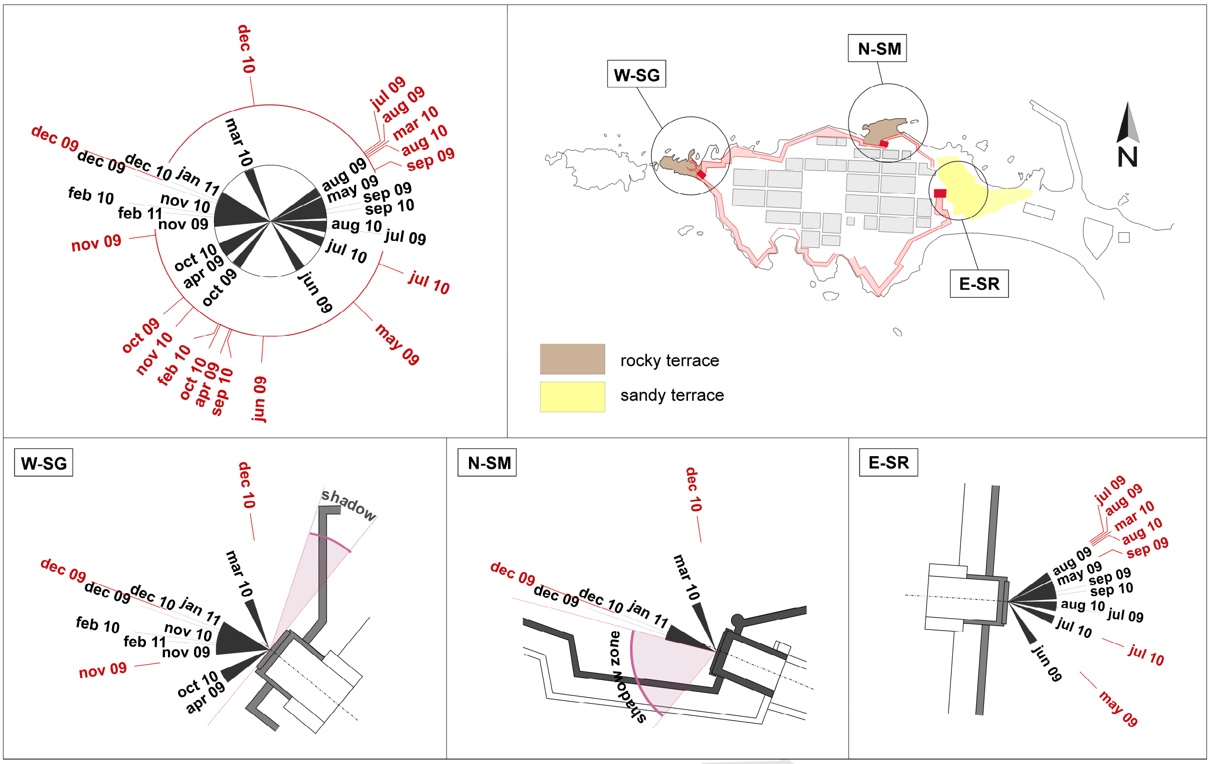
dec 10
jul 09
aug 09
mar 10
aug 10
sep 09
dec 09
dec 09
dec 10
jan 11
mar 10
aug 09
may 09
sep 09
sep 10
feb 10
feb 11
nov 10
nov 09
aug 10
jul 09
nov 09
jul 10
oct 10
apr 09
oct 09
jun 09
jul 10
may 09
oct 09
nov 10
feb 10
oct 10
apr 09
sep 10
jun 09
W-SG
N-SM
E-SR
N
rocky terrace
sandy terrace
shadow
shadow zone

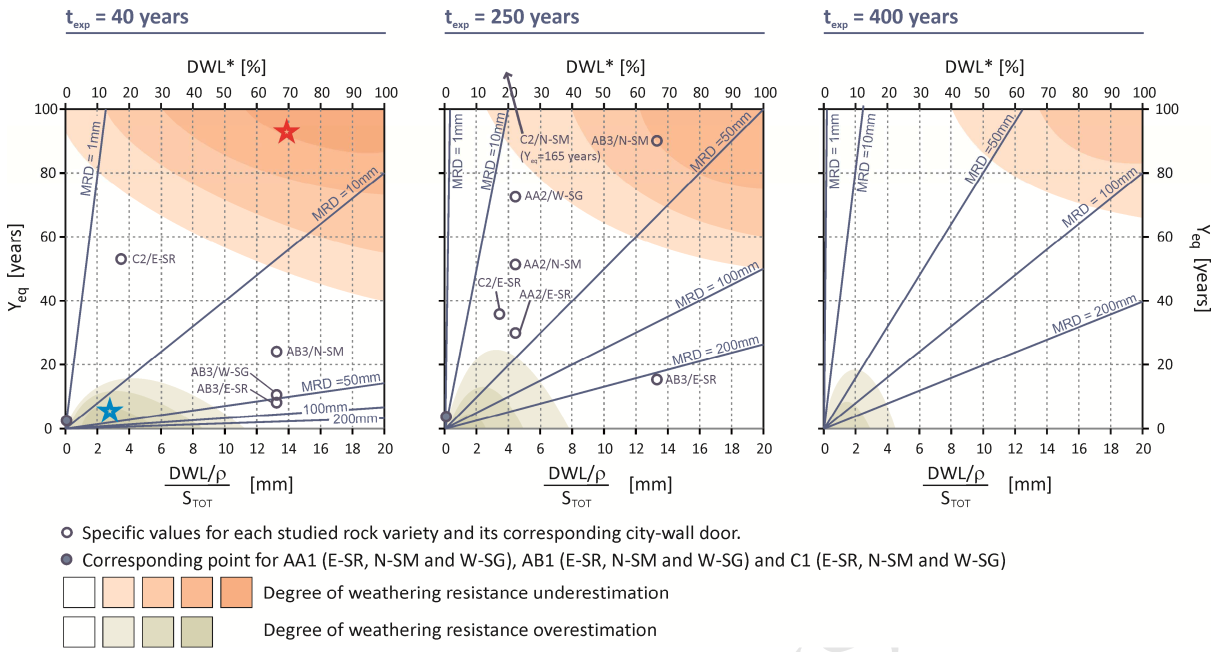

t_exp = 40 years
t_exp = 250 years
t_exp = 400 years
DWL* [%]
Y_eq [years]
DWL/ρ / S_TOT [mm]
MRD = 1mm
MRD =10mm
MRD =50mm
MRD = 100mm
MRD = 200mm
100mm
200mm
C2/E-SR
AB3/N-SM
AB3/W-SG
AB3/E-SR
C2/N-SM
(Y_eq=165 years)
AA2/W-SG
AA2/N-SM
AA2/E-SR
Specific values for each studied rock variety and its corresponding city-wall door.
Corresponding point for AA1 (E-SR, N-SM and W-SG), AB1 (E-SR, N-SM and W-SG) and C1 (E-SR, N-SM and W-SG)
Degree of weathering resistance underestimation
Degree of weathering resistance overestimation

Highlights

- Halite crystallization and wind erosion are reveled as the main weathering agents
- Salt damage depends on both the number and duration of halite transitions
- The location and orientation of monuments control the intensity of stone weathering
- Superficial resistance and porosity determine the durability of rocks
- The representativeness of artificial ageing tests is assessed by a new parameter